Changes in seasonal land precipitation during the latter twentieth-century

K. Noake,[1] D. Polson,[1] G. Hegerl,[1] and X. Zhang[2]

Received 22 November 2011; revised 13 January 2012; accepted 13 January 2012; published 15 February 2012.

[1] Climate models predict substantial changes in seasonal precipitation in the future. Anthropogenic forcing has been found to contribute to the observed pattern of land precipitation change over the 2nd half of the 20th century when annual precipitation is averaged within latitude bands, the observed change was substantially larger than response simulated in climate models, based on a single observational dataset. Here we investigate the robustness of this finding using several land only observational datasets and look for an explanation for why observed changes are significantly larger. We show the discrepancy between model simulated and observed trends is reduced when changes are expressed as percent climatology, which reduces the difference in scale between observed point locations and model gridboxes. Focusing on seasonal rather than annual data reveals that there are seasonal differences in the pattern of zonal precipitation changes over the 20th century. We use fingerprint for zonal precipitation changes from 54 CMIP3 simulations and show that observed changes are detectable in all seasons but boreal summer (JJA), even when doubling the variance of the model simulation, and irrespective of the dataset used. The observed change is still larger than that simulated by the multi-model mean in all datasets except in boreal summer but only in boreal spring is the observed change robustly and significantly larger than that simulated. **Citation:** Noake, K., D. Polson, G. Hegerl, and X. Zhang (2012), Changes in seasonal land precipitation during the latter twentieth-century, *Geophys. Res. Lett.*, *39*, L03706, doi:10.1029/2011GL050405.

1. Introduction

[2] Increased surface temperatures have been observed over the latter half of the 20th century and studies have attributed the majority of this warming to anthropogenic forcing [*Hegerl et al.*, 2007; *Stott et al.*, 2010]. Corresponding to this warming, an increase in moisture content of the atmosphere has been observed [*Santer et al.*, 2007]. In climate model simulations of warming due to CO2 increase, the global precipitation change is smaller than would be expected from the Clausius-Clapeyron relationship. This is because the contribution of latent heat from condensation to the atmosphere's energy budget prevents some of the absolute humidity increase realising as precipitation [*Allen and Ingram*, 2002; *Lambert et al.*, 2004]. Such a constraint does not apply to shortwave forcing, which therefore shows stronger effects on globally averaged land precipitation over the 20th century [*Gillett et al.*, 2004]. Climate models show a robust pattern of zonal precipitation change where wet areas become wetter and dry areas dryer [*Held and Soden*, 2006].

[3] *Zhang et al.* [2007] investigated whether observations show the influence of anthropogenic forcing by analyzing 20th century observations of land precipitation change, averaged within latitude bands, using fingerprints from 14 climate models. They concluded that anthropogenic forcing had contributed to a large part of observed changes and that these changes could not be explained by internal variability or natural forcing. The detected pattern shows increased precipitation in NH high latitudes with decreases north of the equator and increases to the south. The pattern was stronger than expected from the multi-model mean and individual simulations with a best guess scaling factor of 5.8 (5–95% range 2.8–10.9). *Min et al.* [2008] also detected an increase in NH high latitudes precipitation which was stronger than expected from models. Both used a station based gridded dataset of land precipitation. However, observational uncertainty can be substantial [*Zhang et al.*, 2007]. To address it we investigate to what extent findings are sensitive to using different datasets for land precipitation and split results by season to determine more clearly the origin of the enhanced precipitation change relative to the models.

[4] Observed seasonal changes in mean zonal land precipitation are compared with changes simulated by 11 climate models. A total least squares approach, based on the fingerprint detection method [*Allen and Stott*, 2003], was used to detect the influence of external forcings on the observed trends. We did not use optimal detection methods for simplicity and to avoid complicating interpretation by truncating to a low-dimensional space, where not all aspects of the pattern may be represented [see *Hegerl et al.*, 2007].

2. Data and Analysis

[5] Three observational datasets for monthly precipitation were used in this analysis. The datasets include an updated version of data from [*Zhang et al.*, 2007], the VASClimO dataset [*Beck et al.*, 2005], and the Climate Research Unit (CRU) monthly precipitation dataset [*Hulme et al.*, 1998]. The data of *Zhang et al.* [2007] are on a 5 × 5° grid based on long-term stations in the Global Historical Climatology Network (GHCN) monthly precipitation dataset [*Vose et al.*, 1992]. They selected stations with at least 25 years of data during 1961–1990 and at least 5 years of data in every decade during 1950–1999. The updated version replaced

[1]School of GeoSciences, University of Edinburgh, Edinburgh, UK.
[2]Climate Research Division, Environment Canada, Toronto, Ontario, Canada.

0094-8276/12/2011GL050405

Table 1. Scaling Factors From Total and Ordinary Least Squares Fingerprint Methods for VASClimO, Zhang and CRU Observation Datasets[a]

β Season	β TLS	β OLS	5–95% Range 1	5–95% Range 2	r
			VASClimO		
JJA	0.55	0.54	−0.01–1.26	−0.23–1.55	0.47
DJF (without NAO)	1.35	1.31	***0.83–2.05***	***0.62–2.77***	0.69
DJF (with NAO)	1.48	1.41	***0.95–2.20***	***0.74–2.93***	0.65
MAM	2.52	2.26	*1.55–3.93*	*1.28–5.05*	0.70
SON	1.07	1.01	***0.54–2.21***	***0.26–2.82***	0.50
			Zhang		
JJA	1.05	1.02	***0.46–1.73***	***0.23–1.98***	0.58
DJF (without NAO)	1.68	1.57	*1.17–2.40*	***0.98–3.15***	0.65
DJF (with NAO)	1.81	1.66	*1.30–2.55*	*1.11–3.31*	0.62
MAM	3.40	2.64	*2.53–4.78*	*2.53–6.00*	0.59
SON	1.64	1.48	***0.90–2.58***	***0.63–3.21***	0.52
			CRU		
JJA	0.78	0.66	***0.15–1.59***	−0.08–2.01	0.20
DJF (without NAO)	2.52	2.29	*2.08–3.56*	*1.91–4.15*	0.71
DJF (with NAO)	2.72	2.42	*2.28–3.80*	*2.11–4.41*	0.69
MAM	3.56	2.22	*2.37–5.08*	*2.19–6.96*	0.43
SON	2.74	2.27	*2.68–4.49*	*2.53–5.38*	0.57

[a]Range 1 is the total least squares scaling factor uncertainty when climate variability superimposed onto observations and fingerprint, Range 2 is the range resulting from doubling the variance. r is the correlation coefficient for observed and multi-model mean zonal trend patterns.

Canadian stations in the GHCN with adjusted Canadian data [*Mekis and Vincent*, 2011]. The VASClimO dataset consists of 2.5 × 2.5° data from 1951–2000 and is based on quality-controlled and homogenized time-series from 9343 stations. *Hulme et al.* [1998] used station data similar to those in GHCN but a more aggressive spatial interpolation scheme than *Zhang et al.* [2007].

[6] Only gridboxes covered in the *Zhang et al.* [2007] dataset were used and each observation and model dataset were masked to ensure the same coverage in each. Analysis was limited to 40° S to 70° N as observational data elsewhere is too sparse for zonal averages, the data coverage can be seen in Figure 3. We focus on the period 1952–1999 as coverage in the Zhang dataset decreases sharply after 1999, the CRU data stops at 1998, and early 20th century data are sparse. An updated dataset by Zhang extends to 2008, however, with reduced coverage towards the end and shows broadly similar trends to the end of the record (see auxiliary material).[1] We use model data from the WCRP CMIP3 archive, which included 54 simulations from 11 models forced with anthropogenic and natural external forcing to derive a fingerprint of forced change.

[7] Trends were expressed as a percentage change of each latitude band relative to its climatological precipitation rather than absolute values to avoid a mismatch between model gridbox mean and observed data where these are based on only few stations since stations may capture stronger local events. Changes expressed in percent of model climatology were found to be more similar between models than absolute changes. Mean seasonal zonal precipitation change was calculated by averaging absolute monthly precipitation for each season within 5° latitude bands, where seasons were defined as December, January, February (DJF) and each three month period thereafter. Trends were computed by applying a least squares fit to seasonal precipitation averaged for each latitude band and dividing by the mean precipitation for the same period to obtain a percentage change. The multi-model mean trends are the average of all 54 runs.

[8] A total least squares (tls) detection approach was applied to the multi-model mean and observed trends to determine if external influences had caused the changes. This method calculates a fingerprint of external forcing $f_{tot}(x)$ based on the simulated response and applies a least square fit of this fingerprint to the observations $Y(x)$

$$Y(x) = (f_{tot}(x) + \varepsilon_{finger}(x)) \cdot \beta_{tot} + \varepsilon_{noise}(x) \quad (1)$$

where $f_{tot}(x)$ is the mean of the 54 simulated trends over all latitude bands, $\varepsilon_{noise}(x)$ is a residual associated with internal climate variability, $\varepsilon_{finger}(x)$ is variability superimposed on the fingerprint and β_{tot} is the unknown scaling factor which scales the fingerprint of the modelled trend pattern to the observed trend pattern. Here x is latitude.

[9] The tls method is used to reduce the bias due to noise contamination of the fingerprint. However, as there were 54 runs, application of an ordinary least squares method is also justifiable and shown for comparison in Table 1.

[10] For the tls method, noise-reduced observation and model fingerprint are calculated using

$$\widetilde{\mathbf{Z}} = \mathbf{Z} - \mathbf{Z}\widetilde{\mathbf{v}}\widetilde{\mathbf{v}}^T \quad (2)$$

to produce a 'best-fit' of both, where $\mathbf{Z} \equiv [f_{tot}(x), Y(x)]$ and $\widetilde{\mathbf{v}}$ contains the tls coefficients used to calculate β_{tot} [*Allen and Stott*, 2003]. The uncertainty in β_{tot} was evaluated by superimposing samples of noise onto the 'best-fit' observations and fingerprint and recalculating the scaling factor, with the range giving the uncertainty. The samples of random climate variability were calculated by subtracting the multi-model mean trend pattern from each individual model trend and multiplying by a $\sqrt{\frac{n}{n-1}}$ to avoid bias in the variance. Where the 5–95% range of β_{tot} exceeds zero it is concluded that there is a significant ($p < 5\%$) relationship

[1]Auxiliary materials are available in the HTML. doi:10.1029/2011GL050405.

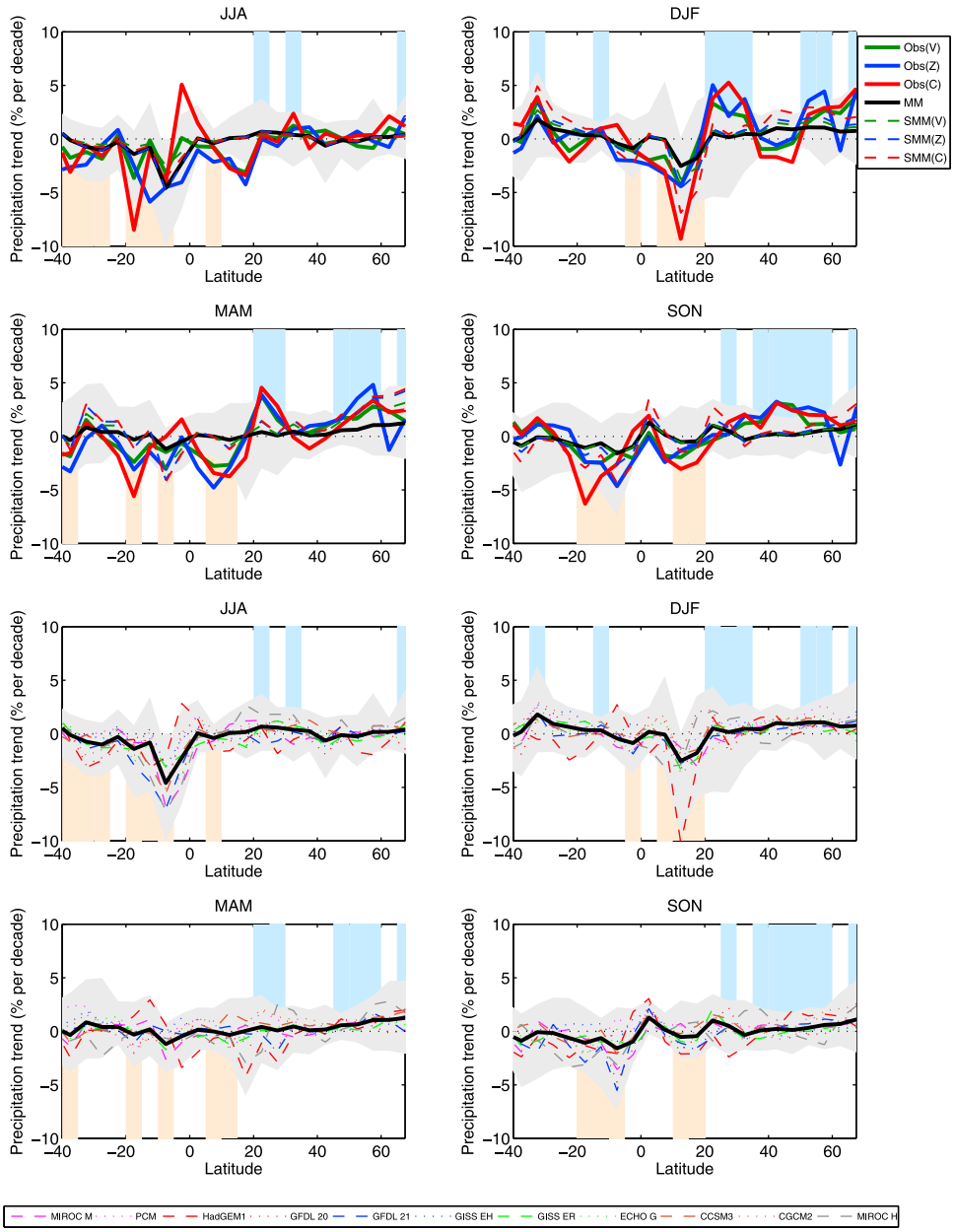

Figure 1. Top four plots show percentage change in observed and simulated zonal mean 3-month season land precipitation for 1952–1999 (1998 for CRU). Solid green, blue and red lines are VASClimO (Obs(V)), Zhang (Obs(Z)) and CRU (Obs (C)) respectively, black line is multi-model mean (MM) and dashed lines are MM scaled by scaling factors for VasClimO (SMM(V)), Zhang (SMM(Z)) and CRU (SMM(C)). Grey area is model 5–95% range, blue and orange areas show where all observations and MM give a positive and negative trend respectively. Bottom four plots show mean trends from individual models compared to MM.

between the observed and multi-model trends that can not be explained by internal climate variability.

3. Results

[11] Latitudinal trends in precipitation were investigated for 1952–1999 for the Zhang and VASClimO data and 1952–1998 for the CRU data. Figure 1 shows the trends for each observational dataset, the model ensemble and multi-model mean. Trends of all observation datasets agree on the broad features of change. Precipitation largely increases poleward of about 50°N in all seasons, particularly during DJF and March, April, May (MAM) [see also *Min et al.*, 2008], with a decrease in the northern tropics, in agreement with expectation and other studies [*Allen and Ingram*, 2002; *Zhang et al.*, 2007]. The June, July, August (JJA) observed trends show a decrease in precipitation north of the equator which includes drying over the Sahel. In MAM there is a dipole around 20°N with a reduction in precipitation to the south similar in magnitude to that of the Sahel and an equally large increase to the north. In addition, precipitation increased poleward of 40°N with the greatest change peaking at 60°N. The September, October, November (SON)

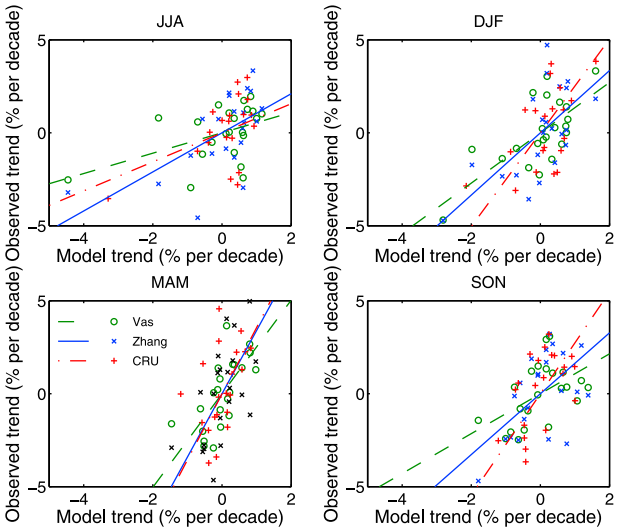

Figure 2. Zonal trends from observations against those from multi-model mean. Latitudinal 3-month seasonal trends are plotted for each 5° band between 40°S and 70°N. Lines indicate the total least square scaling factors between the multi-model mean and observations. DJF trends have influence of NAO removed from observations, but results are not very sensitive to this.

observed trends shows an increase in precipitation over northern mid-latitudes.

[12] To investigate if the trend in the North Atlantic Oscillation (NAO) explains aspects of the observed changes, the precipitation change that is linearly explained by the NAO (Index from CRU [*Jones et al.*, 1997]) was removed from DJF data in the region 35°N to 75°N and 25°W to 40°E, where the influence of the NAO on precipitation was found to be significant ($p < 5\%$) using a Mann–Whitney test [see *Kenyon and Hegerl*, 2010]. The NAO index was detrended prior to regression onto the data to ensure that common trends do not influence the regression. The trends with the influence of the NAO removed reveals the effect is small, with slightly reduced wettening in high latitudes and a neutral rather than slightly negative change at 40°N. The NAO trend between the 1960s and 1990s is therefore unlikely to explain observed trends in NH mid-latitudes (see auxiliary material).

[13] The observed and multi-model mean zonal trend pattern shows moderate agreement with the multi-model mean tending to capture the pattern of change but not the magnitude. Correlations between observed and multi-model mean zonal trends are given in Table 1. DJF has the highest correlations (0.6–0.7) and JJA the lowest (0.2–0.6). The increase in NH mid-latitude precipitation in DJF and MAM is present but underestimated in the models. The model trends also capture changes around the tropics and in the SH in DJF and SON. JJA tends to show least agreement between models and observations, particularly in the Sahel region where the models do not represent the precipitation decrease. The annual trends for the Zhang observations for 1952–1999 and 1952–2008 were calculated and found to be largely consistent with each other and with the trends by *Zhang et al.* [2007] (see auxiliary material). The tls scaling factor of 2.55 (using percentage changes) for the updated 1952–1999 Zhang observations (5–95% range 1.50–3.58) is lower than that of *Zhang et al.* [2007] but still shows a significant underestimation by the models.

[14] Figure 2 shows the observed versus multi-model mean trends for each latitude, emphasising that observations and models tend to agree least in JJA and most in DJF. MAM shows a strong similarity between the pattern of observed and simulated trends, however the multi-model mean greatly underestimates the magnitude of change. The slope of the lines in Figure 2 represent the tls scaling factors in Table 1. From the scaling factors 5–95% range, forcing is detectable in DJF, MAM and SON for all datasets and the scaling factor is smaller than that of *Zhang et al.* [2007] which uses total rather than percentage changes. Scaling factors were also calculated for 1960–99, 1951–90 and 1975–99 and found to be broadly consistent but with wider 5–95% ranges than for 1952–99. The model variability and residuals were compared to ensure the variability is not too small. In general they are similar, however the residuals exceed the model standard deviation by a factor of 2–4 at a few latitudes, mostly in the tropics, for some seasons and datasets. These problem regions are consistent with findings that precipitation variability may be underestimated by models [*Zhang et al.*, 2007]. To address this to some extent, the model variance was doubled (Table 1). Forcing is still detected in all but JJA, but uncertainties remain in our estimate of precipitation variability.

[15] Figure 3 shows the percentage changes in each gridbox for 1952–1999 for JJA and DJF for the VasClimO data. The DJF plot shows the largest percentage changes occurring in the Sahel with substantial decreases in precipitation. The figure shows increased precipitation in northern Europe,

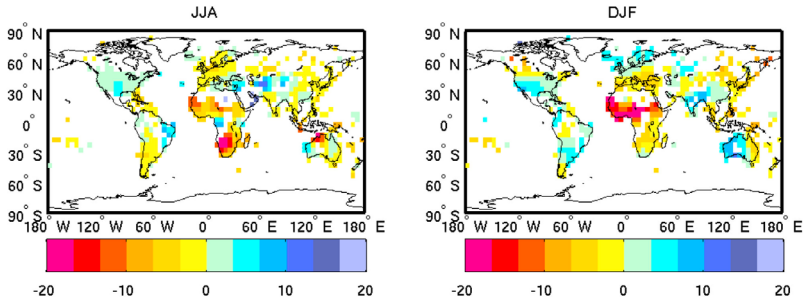

Figure 3. Spatially disaggregated percentage change in precipitation (% per decade) for VasClimO dataset for 1952–1999 for JJA and DJF. Data is smoothed by averaging each gridbox with neighbours. Patterns are similar with the other datasets with some regional differences.

the southern USA, western Australia and Southern Asia. Decreased precipitation is observed in southern Europe, southern Africa, eastern Australia and in the eastern parts of Asia. These same patterns are observed for JJA, however the changes tend to be smaller in many areas, leading to smaller zonal trends in JJA (Figure 1).

4. Discussion and Conclusions

[16] The observed seasonal precipitation trends are robust to the use of different datasets, as is the detection of model trends with external forcing for DJF, MAM and SON. Observed changes show a consistent increase in precipitation in northern mid to high latitudes in all seasons. This finding is largely consistent with modelled changes, although the multi-model mean and individual model means tend to underestimate observed trends. However, the underestimate is robust and significant only in MAM. No in situ measurements of precipitation over ocean are available. Satellite based estimates, which are, however, much shorter and hence should have lower signal-to-noise ratio, find different trends for ocean and land precipitation [*Huffman et al.*, 2009], though over shorter timescales, with positive trends over the oceans in the tropics and a negative, but not statistically significant trend over land [*Gu et al.*, 2007]. The absence of ocean precipitation data may mean we fail to capture a net increase in precipitation in the tropics. The estimates of mean zonal trends are biased towards regions with more observations and these would be substantially improved with the greater spatial coverage provided by satellite data, however the shorter temporal coverage makes it hard to separate signal and noise.

[17] Generally, observed seasonal precipitation changes yield climatologically wet regions wetter, and dry regions dryer. For example, the decrease in precipitation north of the equator, related to the drying over the Sahel is consistent with a southward shift of the ITCZ and previous findings [e.g., *Hoerling et al.*, 2006; *Baines and Folland*, 2007]. The drying over the Sahel is now widely understood as a combination of factors including sea surface temperature changes, reduced vegetation in the region, and possibly aerosols [*Yoshioka et al.*, 2007], but not well captured in the models.

[18] External forcing was detectable in DJF, MAM and SON for all datasets and in JJA for one dataset at the 5% limit. The observations are biased to the NH where changes tend to be less pronounced and less consistent between different observational datasets north of 20°N during the NH summer than other seasons, suggesting the impact of external forcing is less significant during NH summer. Seasonal changes are similar to annual trends by *Zhang et al.* [2007], allowing for differences in the mask and time window. Use of percentage changes shows that model's underestimate of the observed trend may be at least partly explained by scale differences and observational uncertainty. *Zhang et al.* [2007] separated the response of anthropogenic forcing from natural forcing and internal variability and concluded that anthropogenic forcing had contributed significantly to annual changes. It is probable that anthropogenic forcing will have similarly influenced seasonal patterns, however attribution studies are needed to confirm this.

[19] **Acknowledgments.** The authors acknowledge the use of precipitation data of the Climatic Research Unit, University of East Anglia and the VASClimO project, and the modelling groups who contributed to the data archive at PCMDI. This work was supported by the NERC project PAGODA, the National Science Foundation (grant ATM-0296007) and the US Department of Energy's Office of Science and NOAA's Climate Program Office. We also thank two anonymous reviewers for their perceptive and helpful suggestions.

[20] The Editor thanks the two anonymous reviewers for their assistance in evaluating this paper.

References

Allen, M., and W. Ingram (2002), Constraints on future changes in climate and the hydrologic cycle, *Nature*, *419*(6903), 224–232.

Allen, M., and P. Stott (2003), Estimating signal amplitudes in optimal fingerprinting, Part I: Theory, *Clim. Dyn.*, *21*(5), 477–491.

Baines, P., and C. Folland (2007), Evidence for a rapid global climate shift across the late 1960s, *J. Clim.*, *20*, 2721–2744.

Beck, C., J. Grieser, and B. Rudolf (2005), A new monthly precipitation climatology for the global land areas for the period 1951 to 2000, Climate Status Report 2004, German Weather Serv., Offenbach, Germany.

Gillett, N. P., A. J. Weaver, F. W. Zwiers, and M. F. Wehner (2004), Detection of volcanic influence on global precipitation, *Geophys. Res. Lett.*, *31*, L12217, doi:10.1029/2004GL020044.

Gu, G., R. Adler, G. Huffman, and S. Curtis (2007), Tropical rainfall variability on interannual-to-interdecal and longer time scales derived from the GPCP monthly product, *J. Clim.*, *20*, 4033–4046.

Hegerl, G., T. Crowley, W. Hyde, M. Allen, H. Pollack, J. Smerdon, and E. Zorita (2007), Detection of human influence on a new, validated 1500-year temperature reconstruction, *J. Clim.*, *20*, 650–666.

Held, I., and B. Soden (2006), Robust responses of the hydrological cycle to global warming, *J. Clim.*, *19*, 5686–5699.

Hoerling, M., J. Hurrell, J. Eischeid, and A. Phillips (2006), Detection and attribution of twentieth-century northern and southern African rainfall change, *J. Clim.*, *19*, 3989–4008.

Huffman, G. J., R. F. Adler, D. T. Bolvin, and G. Gu (2009), Improving the global precipitation record: GPCP Version 2.1, *Geophys. Res. Lett.*, *36*, L17808, doi:10.1029/2009GL040000.

Hulme, M., T. J. Osborn, and T. C. Johns (1998), Precipitation sensitivity to global warming: Comparison of observations with HadCM2 simulations, *Geophys. Res. Lett.*, *25*(17), 3379–3382.

Jones, P., T. Jonsson, and D. Wheeler (1997), Extension to the North Atlantic Oscillation using early instrumental pressure observations from Gibraltar and south-west Iceland, *Int. J. Climatol.*, *17*(13), 1433–1450.

Kenyon, J., and G. Hegerl (2010), Influence of modes of climate variability on global precipitation extremes, *J. Clim.*, *23*, 6248–6262.

Lambert, F. H., P. A. Stott, M. R. Allen, and M. A. Palmer (2004), Detection and attribution of changes in 20th century land precipitation, *Geophys. Res. Lett.*, *31*, L10203, doi:10.1029/2004GL019545.

Mekis, E., and L. Vincent (2011), An overview of the second generation adjusted daily precipitation dataset for trend analysis in Canada, *Atmos. Ocean*, *49*, 163–177.

Min, S., X. Zhang, and F. Zwiers (2008), Human-induced Arctic moistening, *Science*, *320*(5875), 518–520.

Santer, B., et al. (2007), Identification of human-induced changes in atmospheric moisture content, *Proc. Natl. Acad. Sci. U. S. A.*, *104*, 15,244–15,253.

Stott, P., N. Gillett, G. C. Hegerl, D. Karoly, D. Stone, X. Zhang, and F. Zwiers (2010), Detection and attribution of climate change: A regional perspective, *Wiley Interdiscip. Rev. Clim. Change*, *1*, 192–211.

Vose, R., R. Schmoyer, P. Steurer, T. Peterson, R. Heim, T. Karl, and J. Eischeid (1992), The Global Historical Climatology Network: Long-term monthly temperature, precipitation, sea level pressure, and station pressure data, *Rep. ORNL/CDIAC-53, NDP-041*, Oak Ridge Natl. Lab., Oak Ridge, Tenn.

Yoshioka, W., N. Mahowald, A. Conley, W. Collins, D. Fillmore, C. Zender, and D. Coleman (2007), Impact of desert dust radiative forcing on sahel precipitation: Relative importance of dust compared to sea surface temperature variations, vegetation changes, and greenhouse gas warming, *J. Clim.*, *20*, 1445–1467.

Zhang, X., F. Zwiers, G. Hegerl, F. Lambert, N. Gillett, S. Solomon, P. Stott, and T. Nozawa (2007), Detection of human influence on twentieth-century precipitation trends, *Nature*, *448*(7152), 461–465.

G. C. Hegerl, K. Noake, and D. Polson, School of GeoSciences, Grant Institute, University of Edinburgh, The King's Buildings, West Mains Road, Edinburgh EH9 3JW, UK. (dpolson@staffmail.ed.ac.uk)

X. Zhang, Climate Research Division, Environment Canada, 4905 Dufferin St., Toronto, ON M3H 5T4, Canada.